

Corrosion Protection of Stainless Steel by Double-Layered Oxide Films

Masataka Masuda, Hirotohi Sakamoto, Kohichiro Harada,
and Yasunori Hayashi

*Department of Materials Science and Engineering, Faculty of Engineering, Kyushu University
6-10-1 Hakozaki, Higashi-ku, Fukuoka, 812-8581, JAPAN*

Double-layered oxide films of different pH_{pzc} (pH for point of zero charge) were deposited on stainless steels using RF magnetron sputtering. Anodic polarization measurements in buffer solutions were employed to evaluate the effect of oxide films on the films. The test solution pH was adjusted between the values of pH_{pzc} of both oxides, so one oxide had positive surface charge and the other had negative surface charge. The corrosion behaviors of coated steels were affected by the stacking order of oxide films. The higher pitting resistance was obtained for the specimens of stacking lower pH_{pzc} oxide film as an over layer than an under layer. This was explained by the reason that surface charge of the oxide films affected migration of ions in the corrosive solution. We proposed new method of measuring pH_{pzc} of oxide film with electrochemical AFM (Atomic Force Microscope). The Coulomb force cause by surface fixed charge was detected with AFM in the test solution. This force was varied with the solution pH, and showed minimum value of pH_{pzc} of oxide film. We showed the oxide double-layer of suitable staking order enhanced remarkably the corrosion resistance of the stainless steels.

Keywords : multi-layered film, oxide coating, pH for PZC, EAFM, corrosion protection of stainless steel

1. Introduction

The stainless steels are used in various environments because of their passivation films of the high corrosion resistance. However, the various artificial coatings are examined to use them under more severe environment. The dry coating process attracts attention as the convenient surface treatment method that is available for almost all coating material and substrate material.¹⁾ Especially, the sputtering method is suited to industrialization and to be applicable to the ceramics of high corrosion resistance in the relatively low temperature. However, that the defect exists unavoidably in these coating films has been pointed out. Especially, penetrated pinhole defect of coating film becomes to a starting point of pitting corrosion, and causes the deterioration of coated material quality. The increase of film thickness decreases the film defects, but it is hard to extinguish perfectly the coating film defects. So, the technology that improves corrosion resistance of the coating film including the defects has been demanded. In this paper, we report the effect of the multi layered oxide films on corrosion behavior of stainless steels using rf magnetron sputtering method as an integral part of research regarding the high corrosion resistance of stain-

less steels. Attending to the effect of the surface fixed charge of oxide film in the aqueous solution, we discuss that the multi layered oxide films exert on corrosion resistance. Also, we propose the new measurement method of pH_{pzc} in relation to the surface fixed charge.

2. Experimental

The oxide films were prepared on stainless steel (SUS 304, SUS410) with the RF sputtering apparatus (ULVAC Co. Inc., BC2227). The sputtering targets are Al_2O_3 , SiO_2 , Ta_2O_5 , TiO_2 , and ZrO_2 . The sputtering gas is Ar of the pressure of 5.3Pa and the substrate temperature is 573K. The film thickness is 1 μm . We also prepared multi layered films of oxides to evaluate the effect of the layer on corrosion behavior. The film preparation condition is shown in Table 1.

X ray photoelectron spectroscopy (XPS), and X ray diffraction (XRD), were used for analyzing the oxide film structures.

The critical passivation current density method (CPCD)^{2),3)} was used to evaluate defect area of oxide films. The defect area of oxide films were evaluated with the critical passivation current of anodic polarized steel in 0.5M-

Table 1. Oxide films preparation

Substrates	SUS304, SUS410
Targets	Al ₂ O ₃ , SiO ₂ , Ta ₂ O ₅ , TiO ₂ , ZrO ₂
Formation Condition	Gas Pressure Ar 5.3Pa, RF Power 40 kW/m ² , Substrate Temperature 573 K, Film Thickness 1μm

H₂SO₄+0.05M-KSCN aqueous solution. Also, we evaluated the corrosion resistance of oxide coated steel by the passive current density in sulfuric acid solution without KSCN.

The inductively coupled plasma spectrometry (ICP) analyzed the dissolved ions into the test solution from the oxide coated steels.

We proposed new film defect analyzing method using the liquid crystal.^{4,7)} This method can visualize the defects area with the dynamic scattering mode (DSM) of the nematic liquid crystal. The high voltage was supplied between coated steel and transparent electrode, putting liquid crystal into the gap of steel and electrode. The ion current that flows through film defects causes liquid crystal molecular migration and turbulence of the molecule of the vicinity. This turbulence causes scattering of reflection of light and makes visualize the current flow. We can detect very clearly by microscope as DSM areas are dark parts. We evaluated film defects as the counts of DSM area in the unit area of samples surface.

The anodic polarization measurements were carried out to examine the influence of the layer order of oxide films on the corrosion behavior. The pH of test solution was adjusted to an intermediate value of pH_{pzc} of two oxide films. So, the oxide of less pH_{pzc} had positive surface fixed charge and the other oxide of larger pH_{pzc} had negative value in this test solution. The polarization measurements were carried out with the reference electrode of Ag/AgCl in saturated KCl solution.

Recently, the electric atomic force microscope (EAFM) has been used actively to examine the electrochemistry phenomenon and has generated many interesting results. We made new measurement for pH_{pzc} using the EAFM. The scanning tip of the EAFM was coated with the same oxide film of test steel, and the atomic force was measured as a function of the distance between the tip and the steel. The tip and steel of same oxide films have same sign of surface fixed charge in the test solution. The EAFM measurement detects the combination of atomic force and Coulomb force. The Coulomb force and the atomic force have different formula of a function of distance, so we can easily distinguish the Coulomb force and the atomic

force. As measuring the Coulomb force in the test solutions of various pHs, minimum Coulomb force shows pH for point of zero charge (pH_{pzc}).

3. Results and discussion

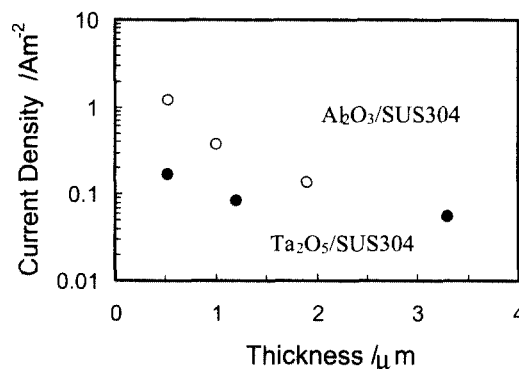
The XPS analysis showed that the chemical composition of oxide films were good agreement with the stoichiometric structure, except of tantalum oxide. The XRD analysis indicated that most of the oxide films were amorphous or fine crystals. The crystal structure that could be confirmed was a poly-crystal and there was no preferred orientation of crystal. The confirmed crystal orientations are shown in Table 2. Tantalum oxide film that consisted of oxygen shortage phase was annealed at 773K in open air for 86.4ks to be transformed into Ta₂O₅ structure. The ICP analysis of the corrosion test solution of coated steel showed only steel was dissolved in the solution and did not detect any element of oxide film in the corrosion solution.

The defect area that calculated by the critical passivation current showed good agreement with the result of liquid crystal method. This result leads that both methods have high reliability to detect of the oxide films defects. The relationship between the critical passivation current and oxide film thickness is shown in Fig. 1. The defects of oxide films decreased with the increase of film thickness obviously.

High: film of higher pH_{pzc}, Low: film of lower pH_{pzc}
The critical passivation current was hardly affected by the kind of oxide film but the passive current density was

Table 2. Lattice index of oxide films.

Oxide	Lattice index
ZrO ₂	$\langle 011 \rangle$, $\langle 111 \rangle$, $\langle 111 \rangle$, $\langle 002 \rangle$, $\langle 211 \rangle$, $\langle 022 \rangle$,
TiO ₂	$\langle 110 \rangle$, $\langle 211 \rangle$, $\langle 220 \rangle$,

**Fig. 1.** Relationship between CPCD and oxide film thickness

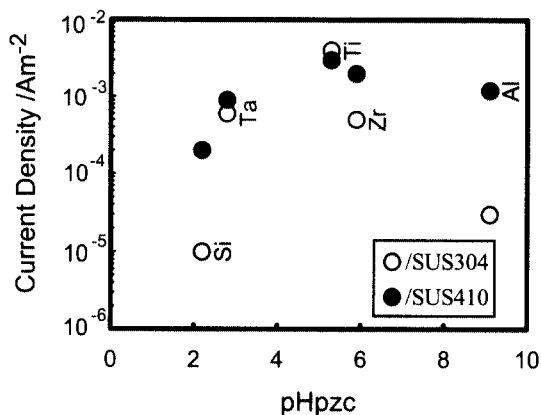


Fig. 2. Relation between passive current density and pH_{pzc} of oxide film

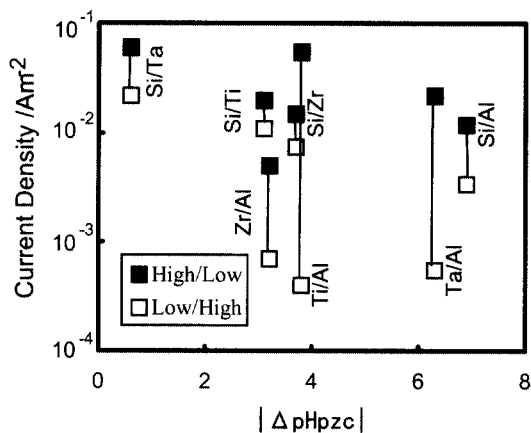


Fig. 3. Relation between passive current density and pH_{pzc} difference of dual-layered oxide film

changed largely by the oxide film type. Fig. 2 shows the relation between passive current density and pH_{pzc} of oxide films. The oxide film of lower pH_{pzc} decreases the passivation current density and shows high corrosion resistance. This phenomenon is explained as the effect of surface fixed charge caused by pH_{pzc} difference. The oxide film of lower pH_{pzc} than the test solution pH gets negative surface charge and the oxide film of higher pH_{pzc} gets positive value. The normal corrosion reaction needs the ion migration of cation from metal to solution and of anion from solution to metal. When the multi layered oxide films of upper layer of lower pH_{pzc} and the lower layer of higher pH_{pzc} were coated, the cation will be prevented to migrate by the lower layer and anion will be prevented by the upper layer.

The ion migration through the oxide film is affected by the surface fixed charge of oxide film. In the case that the lower pH_{pzc} oxide is a top layer and the higher is an under layer, the top layer has negative surface fixed

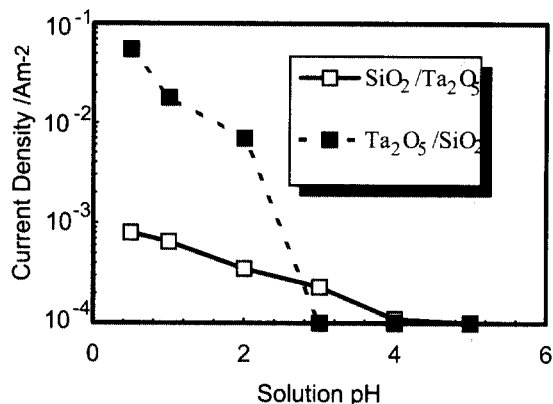


Fig. 4. Behavior of passive current in various solution pH

charge and the under layer has positive charge. The movement of anion is hindered by the top layer charge to migrate from test solution into steel, and the cation is hindered by the under layer to migrate from steel to test solution. And the corrosion current that pass the multi-layered oxide film will decrease. The relationship between the difference of pH_{pzc} of two layered oxides and passive current density is shown in Fig. 3. Obviously, the lower pH_{pzc} oxide film layered over the higher pH_{pzc} oxide has a larger corrosion resistance than the reversely layered oxide films. And the corrosion resistance increases with the increase of the difference between two oxide layer pH_{pzc} . This effect of the difference of pH_{pzc} of oxide films was changed by test solution pH. As shown in Fig. 4, the corrosion resistance of the steel of SiO_2 top layer and Ta_2O_5 under layer was greater than the steel of reversely layered oxides in low pH solution. But the corrosion resistance became almost equal in the higher pH solution as higher pH_{pzc} of oxides. This will be affected by the change of surface fixed charge of two oxide films.

This phenomenon was confirmed in pitting corrosion properties of oxide coated steels. The oxide coated steels polarization curves in buffer solution are shown in Fig. 5.⁸⁾ Al_2O_3 of higher pH_{pzc} and SiO_2 of lower pH_{pzc} were used as coated materials. Three steels showed different pitting potentials. The bare steel had lowest pitting potential, the steel of top Al_2O_3 layer had middle potential, and the steel of top SiO_2 layer had highest pitting potential. The pitting corrosion is generated by the anion condensation, and the ion migration and the condensation are affected by the surface fixed charge of oxide film. Fig. 5 is anodic polarization curves of the multi-layered oxide coated steels measured in buffer solution of $pH=5.4$. Such effect of pH_{pzc} was also seen in the incubation time of pitting corrosion. The incubation time was measured by the break down time of the passivation under constant

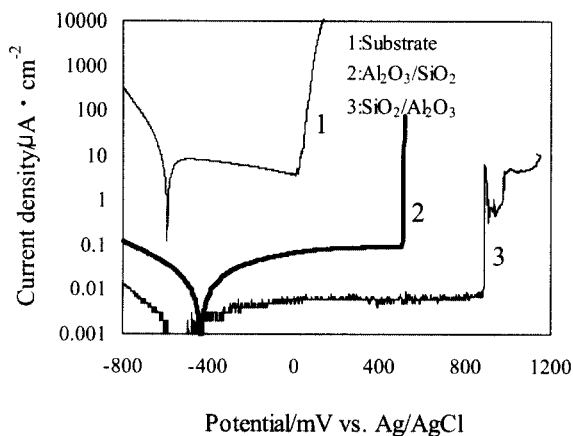


Fig. 5. Anodic polarization curves of the double-layered oxide coated steels measured in buffer solution containing 1.0 kmol/m^3 NaCl of $\text{pH}=5.4$.

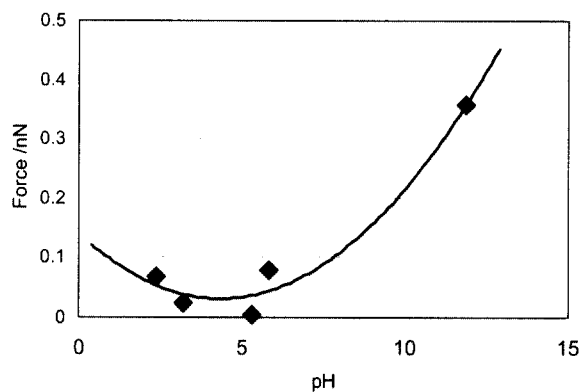


Fig. 6. Relation between repulsive force and solution pH for TiO_2 oxide film

anodic polarization potential in test solution. The incubation time of the steel of the top layer of lower pH_{pzc} oxide was longer than that of the steel of the top layer of higher pH_{pzc} oxide for all couples of oxides coating. Fig. 6 shows the relation between the EAFM force (repulsive force) and the test solution pH for TiO_2 oxide film as distance between the tip and oxide film is constant (5 nm). It is clear that minimum force is given for solution

$\text{pH}=4.3$ and then, the pH_{pzc} of TiO_2 is decided by this value. The EAMF force between the tip and the oxide film includes the atomic force and the Coulomb force. When the Coulomb force has minimum value for pH_{pzc} , the EAMF force shows the minimum value.

4. Conclusions

We evaluated the corrosion resistance of the stainless steel covered with the oxide films by the RF sputtering method. It was shown that the CPCD method quantifies the defect of oxide film and the liquid crystal method visualizes local current flow caused by film defects. The passive current density decreased with the decrease of the pH_{pzc} of oxide film, and the corrosion resistance was improved. In the case of double-layered oxide films of different pH_{pzc} , the steel of the top layer of lower pH_{pzc} oxide had the lower passive current density and had the high corrosion resistance. The steel of the top layer of lower pH_{pzc} oxide had the excellent pitting corrosion resistance. These phenomenon could be explained by the effect by the difference of surface fixed charge whatever. We proposed the new method using electrochemistry AFM to measure pH_{pzc} of oxide.

References

1. K. Sugimoto, N. Hara, and T. Kure, *CAMP-ISIJ*, **7**, 528 (1994).
2. S. Ishiwaka and K. Sugimoto, *JIM*, **51**, 1054 (1987).
3. S. Ishikawa and K. Sugimoto, *Boushoku-Gijyutsu*, **38**, 579 (1989).
4. J. R. Lee, M. Masuda, and Y. Hayashi, *Hyoumen Gijyutsu*, **47**, 76 (1996).
5. J. R. Lee, M. Masuda, and Y. Hayashi, *Hyoumen Gijyutsu*, **47**, 707 (1996).
6. J. R. Lee, M. Kojima, M. Masuda, and Y. Hayashi, *Zairyo-to-Kankyo*, **45**, 23(1996).
7. Y. Hayashi, M. Masuda, and J. R. Lee, *Mater. Sci. Eng. A.*, **198**, 71(1995).
8. K. Harada, M. Masuda, and Y. Hayashi, *Zairyo-to-Kankyo*, **47**, 607(2000).